ULTRASONIC IMAGING OF THE MECHANICAL PROPERTIES OF TISSUES USING LOCALIZED, TRANSIENT ACOUSTIC RADIATION FORCE

Kathryn Nightingale, Mark Palmeri, Kristin Frinkley, Amy Sharma, Liang Zhai, Gregg Trahey

Duke University
Department of Biomedical Engineering
P.O. Box 90281, Durham, NC 27708-0281

ABSTRACT

Acoustic Radiation Force Impulse (ARFI) imaging utilizes brief, high energy, focused acoustic pulses to generate radiation force in tissue, and ultrasonic correlation-based methods to detect the resulting tissue displacements in order to image the relative mechanical properties of tissue. The magnitude and spatial extent of the applied force is dependent upon the transmit beam parameters and the tissue attenuation. Forcing volumes are on the order of 5 mm^3, pulse durations are less than 1 msec, and tissue displacements are typically several microns. Displacement is quantified using interpolation and cross correlation methods. Noise reduction is accomplished by adaptively filtering the temporal response, and median filters are applied to the resulting images. Images of tissue displacement reflect local tissue stiffness, with softer tissues (e.g. fat) displacing farther than stiffer tissues (e.g. muscle). Parametric images of maximum displacement, time to peak displacement, and recovery time provide information about tissue material properties and structure. In both *in vivo* and *ex vivo* data, structures shown in matched B-mode images are in good agreement with those shown in ARFI images, with comparable resolution. Potential clinical applications under investigation include: soft tissue lesion characterization, assessment of focal atherosclerosis, and imaging of thermal lesion formation during tissue ablation procedures. Results from ongoing studies are presented.

1. INTRODUCTION

The use of acoustic radiation force to interrogate the mechanical properties of soft tissues is becoming a widely investigated research area. In general, acoustic radiation force is used to excite tissue, and the tissue response is monitored using either ultrasonic or MR methods [1, 2, 3, 4, 5, 6].

Acoustic Radiation Force Impulse (ARFI) imaging, which is the focus of this paper, uses a commercial diagnostic scanner to generate multiple, short duration radiation forces to interrogate a two-dimensional region of interest, and monitors the tissue response using ultrasonic, correlation-based methods.

This work was supported by NIH grant R01 EB002132-03. We thank Siemens Medical Solutions USA, Inc. for their system support.

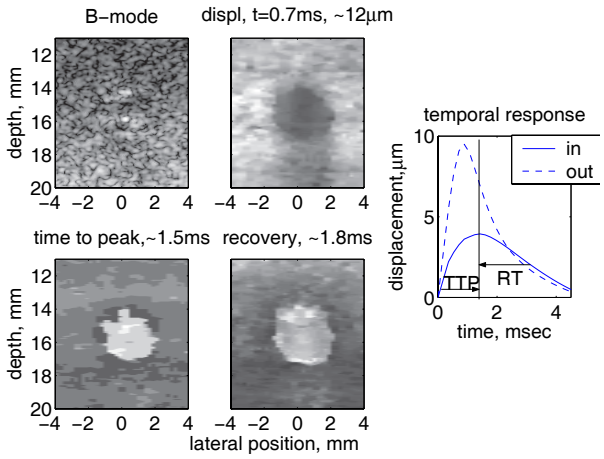

Fig. 1. TOP: Matched B-mode and ARFI displacement images (experimentally acquired) of a tissue mimicking phantom (E=4kPa) with a 3 mm diameter stiffer spherical inclusion (E=15kPa). BOTTOM: Matched experimentally acquired parametric images of the time it took the tissue to reach its peak displacement (TTP,left), and the time it took the tissue to recover from its peak displacement to 63% of its peak value (RT,right) in each spatial location. The plot on the far right portrays the mean response inside and outside the inclusion, showing the smaller magnitude, later peak, and slower recovery of the inclusion that is portrayed in the images.

The mechanical properties of tissue are related to its displacement and recovery response to ARFI excitation. For example, softer tissues move farther than stiffer tissues for a given force magnitude. ARFI imaging has clinical potential in many areas including: identifying and characterizing soft tissue lesions, imaging thermally generated lesions during ablation treatments, characterizing focal and diffuse atherosclerosis, and staging of cancers and poten-

tially lymph nodes of the gastro-intestinal tract.

Because the force application is very short (typically less than 100 μsec), the tissue response is dynamic and effectively portrays the mechanical impulse response of the tissue. In response to ARFI interrogation, most soft tissues exhibit peak displacement magnitudes up to 20 microns, reach their peak displacement in less than 1 msec, and have recovered to their original position within 5 msec. Images of ARFI data are created that portray tissue displacement at a given time, the maximum tissue displacement through all time, the time the tissue takes to reach its peak displacement, and the time it takes the tissue to recover. Given the dynamic nature of ARFI excitation, the tissue response is complicated. Many factors affect tissue behavior including: tissue mechanical, acoustic, and geometric properties, and the magnitude and geometry of the applied radiation force. The region of excitation (ROE) is dictated by the attenuation (α), and speed of sound (c) of the tissue, and the focal characteristics and intensity (I) of the acoustic beam that generates the radiation force [7]: $F = \frac{2\alpha I}{c}$.

ARFI imaging uses higher intensity pulses than conventional B-mode imaging (similar pressure amplitudes, but much longer pulse durations). There are two potential causes of tissue damage during ultrasonic imaging: tissue heating, and cavitation. The MI of the pulses used for ARFI imaging is maintained below the FDA limit of 1.9; thus cavitation should not be a concern. Although the pulse durations are much longer than those used for conventional ultrasound imaging, they are generally less than 100 microseconds. Thus the total amount of acoustic energy is relatively small, as are the associated tissue temperature increases (less than 0.7 °C during a 2-D ARFI interrogation [8]). It is, however, important to evaluate the thermal response of the tissue when designing ARFI sequences.

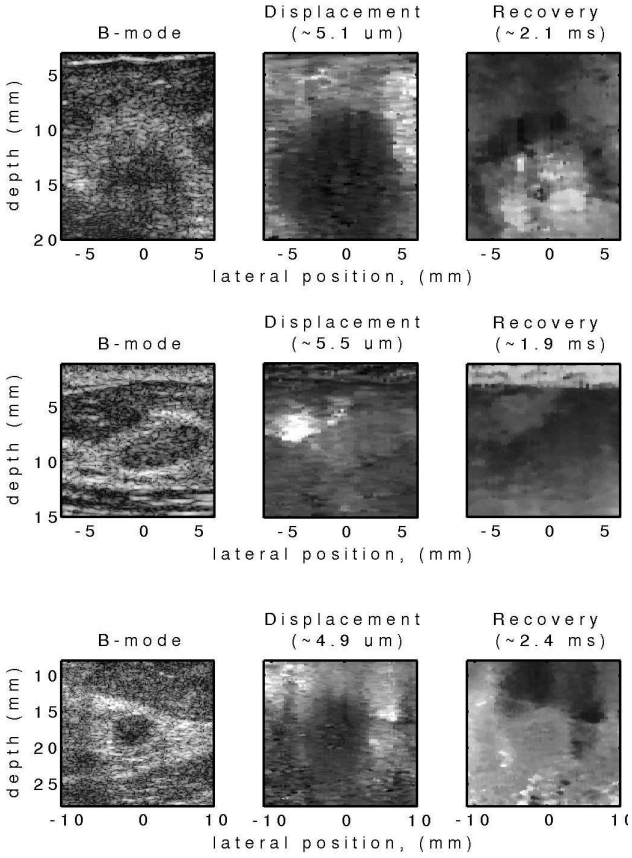

Fig. 2. B-Mode (left), ARFI displacement immediately after force cessation (center), and ARFI recovery (right) images of *in vivo* breast masses from three patients. The ARFI images were generated using multiple focal zones. The mass portrayed in the top row was determined to be malignant upon core biopsy, whereas the mass in the middle row was a fibroadenoma. The mass in the bottom row was also malignant, however it was not as suspicious on the B-mode image. Note that in the malignant cases, the masses appear to have a stiff (darker) boundary in the ARFI displacement image, and appear larger than in the matched B-mode image. In addition, the malignant masses appear to take longer to recover (lighter) then their surrounding tissues. In comparison, the fibroadenoma demonstrates less contrast in the ARFI displacement image than in the matched B-mode image, appears to be fairly homogeneous throughout its extent in the ARFI image, and is unimpressive in the recovery time image.

2. METHODS

ARFI imaging is performed with either a Siemens SONOLINE (TM) Elegra scanner and a 75L40 transducer, or a Siemens SONOLINE (TM) Antares scanner and any number of transducers including: VF105, VF73, CH62, and ER7B (Siemens Medical Solutions USA, Inc., Ultrasound Division, Issaquah, WA). The transducer is selected based upon the application. Both systems have been modified to allow user control of the acoustic beam sequences and intensities, as well as providing access to the raw Radio-Frequency (RF) data.

Beam Sequences: An ARFI imaging system images the mechanical response of tissues to impulsive radiation force excitation. In order to do this, two types of acoustic beams are required: high intensity pushing beams, and conventional B-mode tracking beams. As with conventional ultrasound imaging, data from each look direction is acquired sequentially. In each location, a reference track beam is fired and the received echoes are stored, then a high intensity pushing beam is transmitted that displaces the tissue. This is followed by several track beams to allow observation of the tissue response through time. Typically, a given line of flight is tracked for 5 msec (e.g. 50 A-lines at a PRF of 10kHz). The pushing beams and the tracking beams are co-located. Lateral beam spacing varies from 0.2 to 0.5 mm,

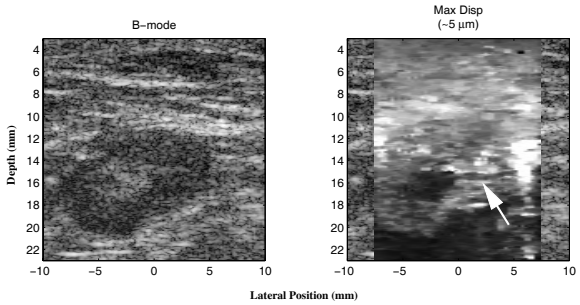

Fig. 3. B-mode (left) and matched ARFI maximum displacement image (right) of an *in vivo*, biopsy-proven reactive lymph node in the breast. The lymph node is the darker oval region in the B-mode image appearing from 12-22 mm in depth. The echogenic center of the lymph node is the normal hilum that corresponds to the region of decreased displacement in the ARFI image (darker region). The node itself appears slightly stiffer (darker) than the surrounding tissue, with a efferent ductal, structure (arrow).

depending upon the desired frame-rate and field of view.

Data Acquisition: For *in vivo* data acquisition, the transducer is hand-held. For *ex vivo* data acquisition, the transducer is held by a ring-stand. Once a region of interest (ROI) is identified using conventional B-mode, the custom pulse sequence is fired and echo data are stored for off-line processing. The RF echo data are obtained by applying depth dependent focal delays to the data received at each active element and summing this data.

Data Processing: Displacement estimates are determined using 1-D cross correlation between sequentially acquired tracking lines [6]. The data is up-sampled both before and after cross correlation. In the *in vivo* images, the temporal displacement profiles are filtered using adaptive eigen filters to reduce noise in the displacement estimates. Finally, the data are spatially median filtered at each time step.

The datasets show tissue displacement through time both during and after force application. The grayscale encoded ARFI images are superimposed over matched B-mode images. In addition to images of tissue displacement, images of the time it takes for the tissue to reach its peak displacement, and tissue recovery time constant are presented (this is defined to be the time it takes the tissue to recover from its maximum displacement to 63% of its maximum displacement).

3. RESULTS

Fig. 1 portrays matched B-mode and ARFI displacement images of a stiff spherical inclusion in a homogeneous background. The plot on the right shows the temporal response of the inclusion, and of the material surrounding the inclusion demonstrating appreciably different behaviors. The inclusion displaces a smaller amount, takes longer to reach its

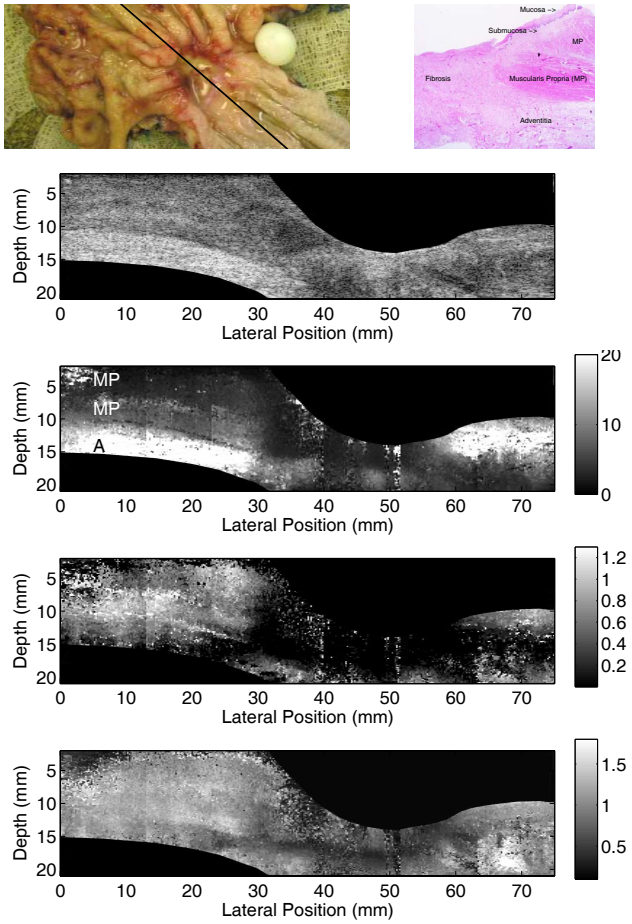

Fig. 4. From top to bottom: Photo of tissue specimen (top left); H&E stain of esophageal side of the ulceration dissected in the imaging plane (top right); Matched B-mode image; ARFI maximum displacement image (Max Disp, microns); ARFI time to peak displacement image (TTP, msec); and ARFI recovery time image (RT, msec) of an *ex vivo*, status post-chemotherapy and radiation, adenocarcinoma in the gastro-esophageal junction. The histologic image demonstrates disruption of the mucosal, submucosal and muscular layers by fibrotic scar tissue. Note the boundary definition in the three visualized layers of the stomach in the ARFI displacement image. Note also the thin black line separating the peri-adventitial tissue from the bottom muscular layer of the muscularis propria, which might be the serosa. The top gel bridge and bottom gauze have been masked in black; Data acquired with the Elegra system, 7.2 MHz center frequency.

peak displacement and recovers more slowly than the surrounding, softer material. This slower behavior of the stiffer inclusion varies with inclusion stiffness and geometry.

Fig. 2 presents matched B-mode and ARFI images obtained *in vivo* in an ongoing pilot study in which images are acquired and correlated with biopsy results. These images demonstrate that B-mode and ARFI images provide complementary information. For the benign mass (middle row), the fibroadenoma exhibits greater contrast in the B-mode image than in either of the ARFI images. However, for the malignant masses shown here (top and bottom rows), the ARFI images demonstrate increased contrast, and portray the mass as larger in the stiffness image than in the B-mode image. In addition, in these examples, the malignant masses demonstrate slower recovery than the surrounding tissue. The larger appearance in stiffness images of some malignant masses has been hypothesized to be due to the body's desmoplastic response to the invading tumor [9].

Fig. 3 presents matched B-mode and ARFI images from the above pilot study obtained in a reactive lymph node, that did not have malignant involvement. The internal structure of the node in the stiffness image demonstrates a stiffer central region with an efferent duct (arrow), which is consistent with normal lymph node structure. The structure is better visualized in the ARFI image than in the B-mode image, and suggests a possible application of ARFI imaging in staging lymph node involvement. We are investigating this application because malignant invasion of lymph nodes generally is initiated along the duct and in the hilum, obliterating these structures.

Fig. 4 presents matched B-mode and ARFI images of an excised gastro-esophageal junction that was excised post-chemotherapy and radiation. The images demonstrate better layer definition in the ARFI images than in the B-mode images, and complete disruption of the layers by the stiffer fibrotic scar tissue is well visualized. These images suggest the potential for ARFI imaging to stage the depth of invasion of tumors of the gastro-intestinal tract.

4. CONCLUSIONS

The work presented herein summarizes results from several ongoing studies of potential clinical applications of ARFI imaging, including breast lesion identification and characterization, and staging of tumors in the gastro-intestinal tract. ARFI images demonstrate excellent axial and lateral resolution: a 3 mm spherical lesion is clearly visualized in ARFI displacement images. The information contained within ARFI images reflects tissue mechanical and geometric properties, whereas B-mode images reflect tissue acoustic properties. ARFI imaging can demonstrate increased contrast over conventional B-mode imaging, and thus may prove a useful adjunct to conventional ultrasonic imaging in several clinical applications.

5. REFERENCES

[1] M. Fatemi and J. Greenleaf, "Vibro-acoustography: An imaging modality based on utrasound-stimulated acoustic emission," *Proc. Natl. Acad. Sci.*, vol. 96, pp. 6603–6608, 1999.

[2] J. Bercoff, M. Tanter, and M. Fink, "Supersonic shear imaging: a new technique for soft tissue elasticity mapping," *IEEE Trans. Ultrason., Ferroelec., Freq. Contr.*, vol. 51, no. 4, pp. 396–409, 2004.

[3] F.L. Lizzi, R. Muratore, C. Deng, J. Ketterling, K. Alam, S. Mikaelian, and A. Kalisz, "Radiation-force technique to monitor lesions during ultrasonic therapy," *Ultrasound Med. Biol.*, vol. 29, no. 11, pp. 1593–1605, 2003.

[4] F. Viola and W. F. Walker, "Radiation force imaging of viscoelastic properties with reduced artifacts," *IEEE Trans Ultrason Ferroelectr Freq Control*, vol. 50, no. 6, pp. 736–742, Jun 2003.

[5] A. Sarvazyan, O. Rudenko, S. Swanson, J. Fowlkes, and S. Emelianov, "Shear wave elasticity imaging: A new ultrasonic technology of medical diagnostics," *Ultrasound Med. Biol.*, vol. 24, no. 9, pp. 1419–1435, 1998.

[6] K. Nightingale, R. Bentley, and G.E. Trahey, "Observations of tissue response to acoustic radiation force: Opportunities for imaging," *Ultrasonic Imaging*, vol. 24, pp. 100–108, 2002.

[7] W.L.M. Nyborg, "Acoustic streaming," in *Physical Acoustics*, W.P. Mason, Ed., vol. IIB, chapter 11, pp. 265–331. Academic Press Inc, New York, 1965.

[8] M.L. Palmeri and K.R. Nightingale, "On the thermal effects associated with radiation force imaging of soft tissue," *IEEE Trans. Ultrason., Ferroelec., Freq. Contr.*, , no. 5, pp. 551–565, 2004.

[9] B. Garra, E. Cespedes, J. Ophir, S. Spratt, R. Zuurbier, C. Magnant, and M. Pennanen, "Elastography of breast lesions: Initial clinical results," *Radiology*, vol. 202, pp. 79–86, 1997.